Theoretical Investigation of One-Dimensional Cavities in Two-Dimensional Photonic Crystals

Stavroula Foteinopoulou and Costas M. Soukoulis

***Abstract*—We study numerically the features of the resonant peak of one-dimensional (1-D) dielectric cavities in a two-dimensional (2-D) hexagonal lattice. We use both the transfer matrix method and the finite difference time-domain (FDTD) method to calculate the transmission coefficient. We compare the two methods and discuss their results for the transmission and quality factor Q of the resonant peak. We also examine the dependence of Q on absorption and losses, the thickness of the sample, and the lateral width of the cavity. The Q-factor dependence on the width of the source in the FDTD calculations is also given.**

***Index Terms*—Cavity, photonic crystals, quality factor, resonance.**

I. Introduction

IN SEMICONDUCTOR crystals, the presence of the periodic potential affects the properties of the electrons. Likewise in photonic crystals (PCs) that are periodic dielectric arrangements in one, two, or three dimensions, the properties of the photon can be controlled. For certain frequency regions known as "the photonic bandgap," propagation of electromagnetic waves is prohibited in the PC [1]–[4]. A defect present in an otherwise periodic crystal may introduce one or more propagation modes in the bandgap and forms a cavity. Cavities of different geometries can exist in a PC and the resulting resonant mode can be classified into two general types indicating whether it drops from the "air" (higher) band or raises from the "dielectric" (lower) band [5]. The first type is associated with defects corresponding to the removal of dielectric material while the second corresponds to defects involving the addition of dielectric material. The features of the resonant mode will depend on both the bulk crystal and the cavity characteristics and can so be tuned accordingly [1]–[3], [5].

An important virtue of the PC cavity is that it can control the atomic spontaneous emission, while metallic cavities for the related frequency range are generally lossy [6]–[8]. Spontaneous emission is important for a number of semiconductor devices [9]. Resonant cavities have undergone extensive studies [8], [10]–[13], both theoretical and experimental. A variety of applications incorporating a PC cavity have been suggested or reported [14]–[16], such as optical laser components [1]–[3], optical filters [5], single-mode light-emitting diode [9], [17], and optical imaging [18].

In this paper, we focus on the theoretical study of an 1-D dielectric cavity in between a hexagonal patterned region of air cylinders in a dielectric matrix for the case of H polarization (magnetic field along the cylinder axis). We will present the cavity mode frequency versus the cavity length (L_c) (see Fig. 1), as well as the quality factor (Q) of the modes versus their corresponding frequency. The quality factor is defined as $\lambda_p/\delta\lambda$ where λ_p is the frequency of the resonant peak and $\delta\lambda$ is the width of the resonance at transmission half of its maximum value. In our case, the quality factor Q of the resonance is relatively small ($\sim$200), and other methods of determining the Q factor (such as from the energy decay of the resonance [19]) give similar results. The dependence of the resonant mode on the size of the system (in the lateral direction and in the direction of propagation) will be also shown. In our calculations, two different numerical techniques (the transfer matrix and the FDTD) are used and the results of the two methods are compared and discussed. With both techniques, we calculate the transmission through the structure and from that we obtain all the relevant features of the resonant mode.

In Section II, we describe briefly the two calculational methods. In Section III, we present and discuss our calculational results concerning the quality factor and position of the cavity resonance. We also compare the latter with the values obtained from the experiment previously performed on the structure under study [20]. In Section IV, we give a summary of our results.

II. Calculational Methods

The first technique we use is the transfer matrix method (TMM) developed by Pendry [21], [22]. In the TMM, a grid lattice is used to discretize the space, and the structure is divided into finite blocks along the propagation direction. With the use of Maxwell's equations, that are solved on the grid lattice, the electric and magnetic field can be integrated throughout the blocks and so the respective transmission coefficient can be calculated. The final transmission will result by combining those for the individual blocks. In the TMM, the modeled structure is finite in the propagation direction (y) but infinite the x, z directions (where z is the direction of the air cylinders), and the incoming electromagnetic wave is a plane wave. The structure is embedded in a medium with a dielectric constant equal to the background dielectric constant to simulate the experiment [20].

Manuscript received September 10, 2001; revised January 24, 2002. This work was supported by the IST Project PCIC of the European Union and by the National Science Foundation under Grant INT-0001236. Ames Laboratory is operated by the U.S. Department of Energy by Iowa State University under Contract W-7405-Eng-82.

S. Foteinopoulou is with Ames Laboratory–USDOE and the Department of Physics and Astronomy, Iowa State University, Ames, IA 50011 USA.

C. M. Soukoulis is with the Ames Laboratory–USDOE and the Department of Physics and Astronomy, Iowa State University, Ames, IA 50011 USA, and also with the Research Center of Crete-FORTH and the Department of Physics, University of Crete, Heraklion, Crete 71110, Greece.

Publisher Item Identifier S 0018-9197(02)05697-X.

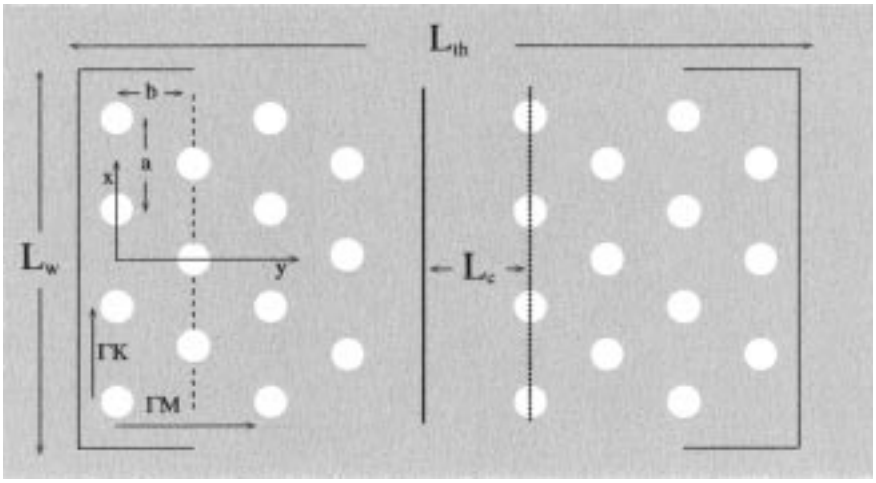

Fig. 1. The cavity structure under study. The bulk crystals symmetry directions ΓM and ΓK are shown. L_c refers to the cavity width. For the actual crystal, $2b = \sqrt{3}a$, but in the TMM, due to necessary approximations, $2b = 1.7a$. L_w is the lateral width of the cavity while L_{th} is the thickness of the cavity system.

The second method we use is the finite-difference time-domain (FDTD) technique [19], [23]. The real space is discretized on a grid lattice and Maxwell's equations are solved in the time domain. The electric and magnetic fields are updated in every point of the grid lattice in finite time steps. The structure is infinite in the direction of the cylinders (z direction) but has finite size in both the x and y directions and is embedded in a finite sized (in x and y) dielectric slab with a dielectric constant equal to that of the matrix medium. Liao absorbing boundary conditions [24] are applied at the walls of the slab to avoid reflections. The source is a pulse, located close to $x = 0$, $y = 0$ (y being the direction of propagation), has a finite length, and generates fields with a trapezoidal (extended with Gaussian tails) profile in space. To calculate the transmission, a line detector is placed along the lateral direction after the structure. The component that is perpendicular to the detector of the Poynting vector (for the Fourier transformed fields) is taken and averaged over the detector. This is normalized with the respective value for the same detector but positioned close to the source in the absence of the structure (to avoid corrupting the data with reflections) and yields the transmission of the structure.

In both methods the quality factor is calculated from the transmission versus frequency data from $\lambda_p/\delta\lambda$ where λ_p is the frequency of the resonant peak and $\delta\lambda$ is the width of the resonance at transmission half of its maximum.

The two methods differ not only in the calculational approach but also in the characteristics of the source of the incoming EM waves, and in the lateral size of the sample that is simulated. We also performed calculations using the FDTD method but applying Bloch (periodic) boundary conditions in the lateral (x) direction to have conditions similar to those for the transfer matrix. The source that is used in the latter case is still a pulse but with a plane-wave front.

III. Results

In Fig. 1, the cross section of the cavity structure under study with the x–y plane can be seen. It corresponds to air cylinders ($\epsilon_a = 1.0$) in a GaAs background ($\epsilon_b = 11.3$) (the value of the GaAs dieletric constant for ~1000 nm is assumed in the calculations for simplicity). The whole cavity structure is embedded in GaAs ($\epsilon = 11.3$). The symmetry directions of the bulk crystal are also shown. With L_c, we will refer to the cavity width that corresponds to the length of the dielectric defect introduced along the propagation direction. With L_w, we will refer to the lateral width of the cavity (which is the same as the sample's lateral width). N_c will be the number of rows on each side of the cavity ($N_c = 4$ for both calculations and experiment). The thickness of the sample then along the propagation direction would be $L_{th} = 2N_c b + L_c$, where $2b = \sqrt{3}a$ (but is approximated with $1.7a$ in the TMM for numerical reasons). (Such an approximation introduces an error of at most 3% in the position of the resonance and does not affect the quality factor.) The radius R of the air holes is $R \sim 0.2803a$ (a being the lattice constant) that corresponds to a filling factor of ~0.285. (Actually in the TMM because of the approximation mentioned above the simulated structure will have a slightly larger filling factor). No specific value for the lattice constant a is assumed. All of the band gap and transmission properties in a PC scale with the lattice constant a, so all the subsequent results will be presented in dimensionless units of frequency (reduced frequency $u = a/\lambda$) and length.

From the transfer matrix results for the various L_c, we observed that the spectral gap when the cavity is introduced is wider than the one for the periodic crystal. Such widening of the gap was also observed in [13] when a defect is introduced by removal of two rows of sites in a periodic 2-D system of dielectric rods in air background. TMM calculations have been performed for cavity structures with dimensionless L_c/a ranging from ~0.15 to 2.0. At a certain frequency, different resonances (peaks) can occur corresponding to different L_c values. Each of these peaks is characterized by an order that basically indicates the order at which a resonant peak appears at this specific frequency while L_c is increasing.

In Fig. 2, every cavity width (in units of a) is plotted as a function of the corresponding reduced frequency of the observed peak and three different curves are recovered for the three orders of the resonant peaks. Starting from the lower to

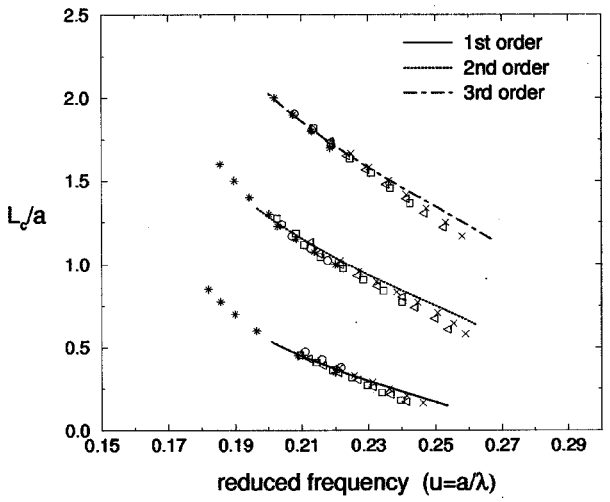

Fig. 2. Cavity width versus the reduced frequency of the corresponding observed cavity resonant peaks. The results are obtained with the TMM (solid dotted and dot-dashed line). The experimental results for various lattice constants a are shown for comparison. The stars, circles, squares, triangles (left), and x are for $a = 200$, 210, 220, 230, and 240 nm, respectively.

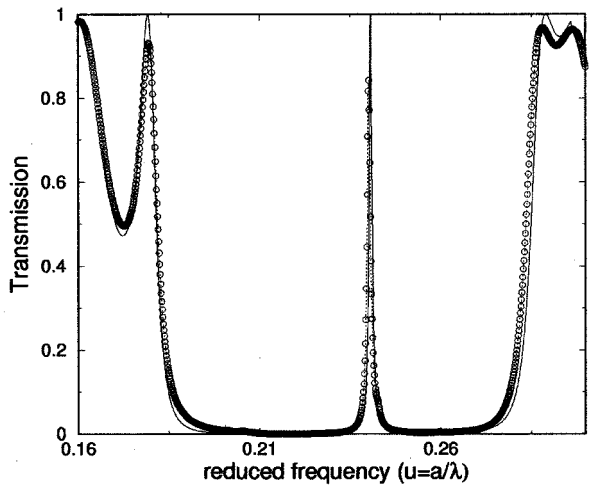

Fig. 3. Comparison between transmission results obtained with the TMM technique (solid line) and the FDTD (dotted line with circles), for $L_c/a = 0.85$. In order to make the comparison in this particular case, we considered an approximate triangular structure $(2b = 1.7a)$ in the FDTD method too.

the higher curve in Fig. 2, the peaks are the first-, second-, and third-order, respectively. It will be seen later that peaks of the same frequency but different order can have different features (e.g., quality factor). It is evident from Fig. 2 that for certain L_c values more than one resonant peak can appear within the gap. The experimental results [20] for the resonant peaks for various lattice constants ($a = 200$ nm, 210 nm, 220 nm, 230 nm, 240 nm) are also included in the figure. The agreement is generally good but there seems to be a small discrepancy that increases with the frequency. This can be attributed to the fact that we have taken the GaAs dielectric constant not to vary with the frequency (for simplicity the value at $\sim$1000 nm is taken in our calculations) while this is not the case in the actual system. This difference in the dielectric will slightly alter the position of the peaks [20]. This is consistent with the fact that the discrepancy at the higher end of the reduced frequencies seems to be a little larger for the smaller lattice constant (the corresponding wavelength differs more from the value of a 1000 nm). There are also some experimental peaks for $a = 200$ nm that are falling above the theoretical curves as, for example, the first-order peaks with L_c/a from $\sim$0.60 to 0.85. We have not numerically calculated the Qs for these, because they lie too close to the band edges and the determination of their quality factor can be vague and so we have not included them in Fig. 2.

We compare now the two computational methods (TMM and FDTD) that are used to simulate the cavity structure. There are basically three fundamental differences between the two methods. The first one is that the transfer matrix technique is a time-independent method while for FDTD the fields are solved in time domain. Also, in the TMM, the structure is infinite in x by virtue of the periodic boundary conditions applied along this direction, while in the FDTD the system is finite in the x–y plane bounded by the absorbing boundary conditions. Finally, the incoming electromagnetic fields in the TMM framework are extended plane waves incident on the whole x–z boundary (corresponding to a source infinite in width) while in the FDTD a pulse emitted from a source with finite width is considered. Also, the way the transmission coefficient is obtained is different in the two methods. In the TMM, it is calculated from the transfer matrix using the field values while in the FDTD it is calculated from the energy ratio that passes through the crystal along the propagation direction. In order to make the comparison between the two methods in this particular FDTD calculation, the 2-D space is discretized as in the transfer matrix which gives $2b = 1.7a$ instead of $\sqrt{3}a$. The results for one particular cavity width are shown in Fig. 3. Good agreement is found between the two methods regarding the positions of the resonant peak and the bandgap edges but there is a small discrepancy in the quality factor of the peak.

It is interesting therefore to see how the quality factor of the resonant peak is affected by the finiteness of the size of the system and the width of the source, in our FDTD calculations. This can be seen in Fig. 4(a) and (b) where the quality factor versus the lateral width of the sample (L_w) and versus the source width are shown, respectively. In Fig. 4(a), the ratio of the source width over the lateral extent of the structure L_w (defined in Fig. 1) is kept constant (equal to 0.5). It can be seen that, as the lateral width approaches $20a$, Q saturates at a value $\sim$170. In Fig. 4(b) we present results of the Q versus the source width for a system with a lateral width of $L_w = 40a$. The width L_w is large enough for the quality factor to have reached its saturation value (which is related to the lateral size) so that one can see the dependence on the source width only. It is clearly seen that for a small source width the quality factor drops significantly. From the data shown in Fig. 4(a) and (b), it can therefore be argued that the finiteness of the source or the system's lateral size or both give 2-D characteristics in what would essentially be a 1-D resonance for the infinite system and result in a reduced quality factor. By an infinite system, we mean an infinite lateral size and that the incoming waves have a plane wave front. In our system, when the lateral size is small the resonance is supported by a smaller number of scatterers and is forced to

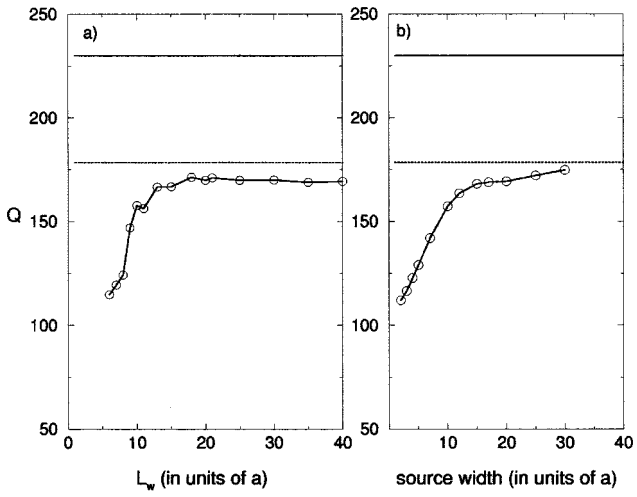

Fig. 4. (a) Quality factor Q for a structure with a width $L_c/b = 1.(2b = \sqrt{3}a$ is taken) calculated with the FDTD versus L_w (in units of a) (see Fig. 1). The source is chosen to have a length approximately half of the lateral length of the structure for all L_w. (b) Quality factor Q calculated with the FDTD (solid line with circles) with the same L_c/b as in (a), versus the source width (in units of a). L_w is kept constant and equal to $40a$. In both (a) and (b), the bold dotted line represents the value of the quality factor calculated with the same method but with periodic (Bloch) boundary conditions along the lateral direction (i.e., perpendicularly to the propagation direction). The source used in the calculations corresponding to that case is a pulse but with plane wave front. The horizontal solid line is the TMM result.

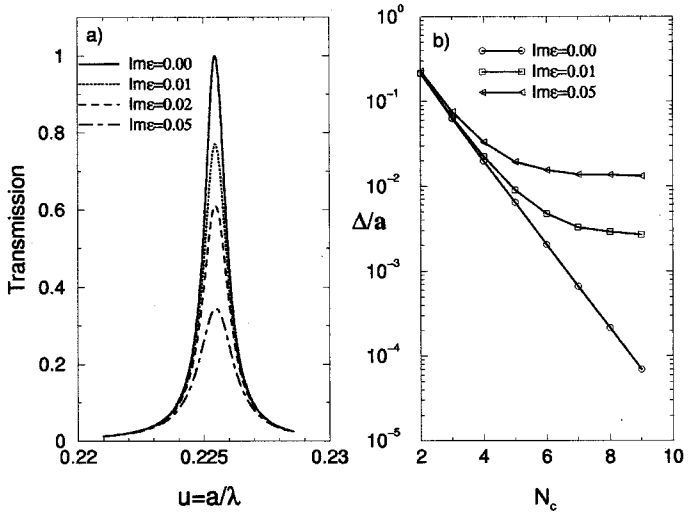

Fig. 5. (a) Transmission calculated by the TMM versus reduced frequency $u = a/\lambda$ for different values of Im ϵ of the air dielectric. $L_c/a = 0.985$ on the cavity resonance (for $N_c = 4$). (b) Dimensionless linewidth (Δ is $\delta\lambda$ i.e., the wavelength width that corresponds to transmission half of the peak's maximum) versus N_c (number of rows in each side of the cavity) for the lossless case as well as the cases with nonzero imaginary part in the air dielectric constant.

terminate at the edges. Also, when the system is large but the source is small, the resonance occupies a smaller fraction of the cavity area and has a magnitude that decreases as one moves away from the center of the resonance. The resonance can decay in time not only along the propagation direction y, as the true 1-D resonance does, but also along the lateral direction. In both cases (small lateral width or small source), the result would be a smaller quality factor. Now, for the case when both the system and the source are very large, the resonance can be extended in the cavity region and be very close to the 1-D resonance. As seen in Fig. 4(b), for a source width equal to $30a$ and $L_w = 40a$, the quality factor is $\sim$174. That value is close to $\sim$180 which is the value of the quality factor as obtained from the FDTD that models the infinite system (Bloch boundary conditions) (dotted horizontal line in Fig. 4). The solid horizontal lines in Fig. 4(a) and (b) give the quality factor for the infinite system as obtained from the TMM. The respective value is $\sim$230. We have also looked at the dependence of the quality factor on the lateral width and kept the width of the source constant and equal to $2a$. What we found was that the quality factor increases as the lateral width increases, reaches a maximum value, then starts to decrease and eventually saturates. This is the result of a combined effect. As described previously, when the lateral width is small this causes the resonant peak to terminate at the edges. As the lateral width increases, the resonance occupies the maximum area it can—according to the specific source width. Increasing further the lateral width will not cause the resonance to occupy more of the cavity along the lateral direction x. It only allows it to decay in time along the x direction as well and therefore the quality factor starts to lessen.Another component that can cause the quality factor to decrease with decreasing source width is the angle span of the source that increases with the decreasing source width. This would cause the peak to shift and broaden (toward the higher frequencies). We have numerically checked that the magnitude for the off-normal components of the incoming wave is relatively small. Also, we have not observed significant shift in frequency with decreasing source width in the FDTD results. We have observed though that the height of the transmission peak decreases as the source width decreases. It approaches the value of one as the source width approaches the lateral size of the system (for the large system $L_w = 40a$). It becomes one for the infinite system modeled either through the TMM or the FDTD with Bloch boundary conditions in the lateral direction of the crystal.

Fig. 5(a) shows the transmission calculated with the TMM method versus the reduced frequency $u = a/\lambda$ for a 1-D cavity of width $L_c/a = 0.985$ and $N_c = 4$, for different imaginary parts in the air dielectric constant. Introducing imaginary parts with values of 0.02–0.05 in the air dielectric constant in the TMM system, has been suggested as a mechanism to model out of plane losses in [20]. This leads as well to a reduced Q factor value. N_c is the number of rows of air cylinders in each side of the 1-D dielectric cavity. As expected the transmission peak decreases with Im ϵ while the width of the transmission increases with Im ϵ. We have also examined how the size of the system along the propagation direction affects the characteristics of the resonance. In Fig. 5(b), the dimesionless linewidth Δ/a—which is defined as $\delta\lambda/a$ (where $\delta\lambda$ is the width in wavelength of the resonance at the half maximum value)—is plotted versus N_c (the number of rows of cylinders on each side of the dielectric cavity) on a semi-logarithmic scale. As mentioned previously, N_c is related to the thickness of the system $L_{\rm th}$ through the relation $L_{\rm th} = 2N_c b + L_c$ ($L_{\rm th}$ is shown in Fig. 1).

A linear relation on the semi-log scale between Δ/a with N_c is obtained, meaning that the quality factor Q, which is inversely proportional to Δ/a, would increase exponentially with

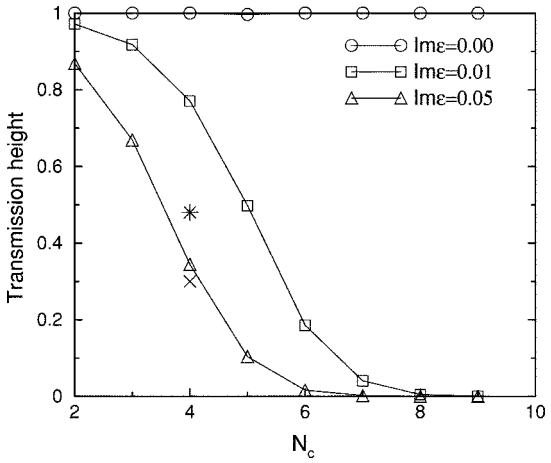

Fig. 6. Transmission height of the resonance for $L_c/a = 0.985$ for three values of the imaginary part of the air dielectric constant, $\mathrm{Im}\,\epsilon$. Two experimental values for the cavity with $N_c = 4$ are shown for comparison. The star and x correspond to $a = 230$ nm with $L_c/a = 1.07$ and $a = 220$ nm with $L_c/a = 0.98$, respectively.

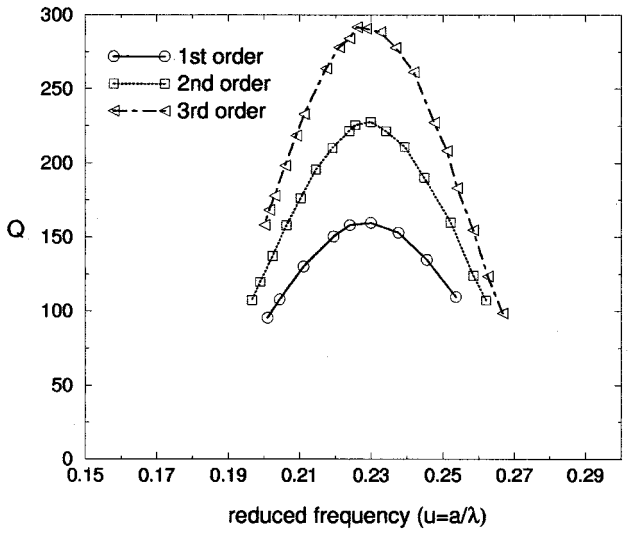

Fig. 7. Quality factor calculated with the TMM versus the reduced frequency for first-, second-, and third-order resonant peaks.

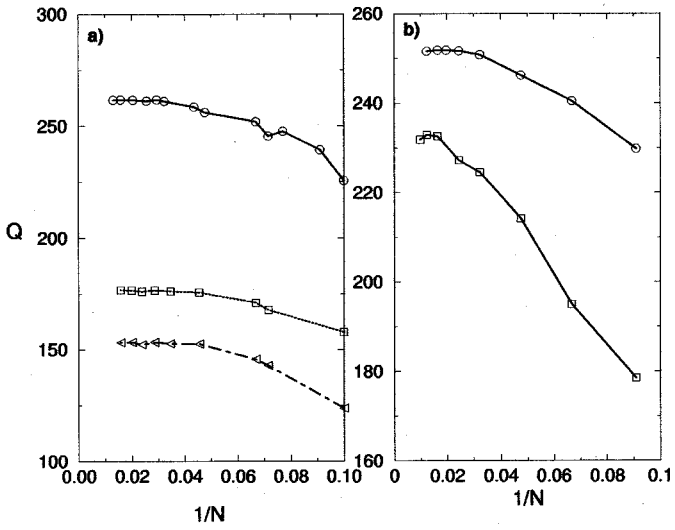

Fig. 8. (a) Quality factor for three different cavity peaks with reduced frequencies $u = 0.2255$ (solid line), $u = 0.2063$ (dotted line), and $u = 0.2628$ (dotted-dashed line) versus $1/N$, where N is the number of grid spacings that the lattice constant a is divided into in the computation. The peaks at $u = 0.2255$ and $u = 0.2063$ are second-order peaks and have $L_c/a = 0.985$ and $L_c/a = 1.2$, respectively. The peak at $u = 0.2628$ is of third order (with $L_c/a = 1.2$). The quality factor saturates at a value as the numerical accuracy of the method increases. (b) Quality factor for $Lc/b = 1$. As a function of the grid accuracy calculated from the FDTD method with Bloch boundary conditions across the lateral direction (solid line with squares) and from the TMM (solid line with circles).

N_c. That is consistent with the results for other defect cavities [13], [25]. In Sigalas *et al.* [13], where an air defect in a dielectric array is studied, it was shown that when absorption is introduced in the dielectric the quality factor saturates and does not increase any further as the size of the system increases. Such saturation with the introduction of an imaginary part in the dielectric of the holes is observed in our case also, as can be seen in Fig. 5(b). We also observe (as in [13]) that the saturation value of the linewidth Δ is smaller, the larger the imaginary part in the dielectric.

In Fig. 6, we present the results achieved with the TMM of the transmission height versus N_c for a 1-D cavity of width $L_c/a = 0.985$ for three different values of $\mathrm{Im}\,\epsilon$ of the air dielectric. Notice that for $\mathrm{Im}\,\epsilon = 0$ the height is always one, i.e., perfect transmission. However, for a nonzero value of $\mathrm{Im}\epsilon$, the transmission height drops as N_c increases. Two experimental values are shown for almost the same width of L_c/a as the one in the calculations. Notice that this suggests that the $\mathrm{Im}\epsilon$ that can fit the experimental data [20] can have a value close to 0.04.

For the ideal case with no losses present, the quality factor was calculated by the TMM for various cavity widths L_c that led to peaks that span most of the bandgap. In Fig. 7, the quality factor is plotted versus the reduced frequency of the peak. (Peaks too close to the edges of the bandgap were not used because the determination of their Q would be vague as stated earlier in this paper). For every frequency in the plot, there are three peaks that are characterized by different orders and correspond to different L_c values (see Fig. 2). So three different curves are recovered when grouping the peaks according to order. Higher order peaks are characterized by a higher value of the quality factor. For every order, the quality factor is maximum for a frequency close to the center of the bandgap and reduces as the frequency approaches either edge of the bandgap. The calculations above were performed with a grid lattice dividing the lattice constant a into ten intervals. We have investigated the dependence of the quality factor with the accuracy of the TMM given by the number N of intervals the lattice constant is divided into, i.e., N is the number of grid points. It was done for three different peaks. One close to the band gap center and the others close to the lower and higher frequency band edge respectively. It is seen from Fig. 8(a) that the quality factor increases with increasing accuracy and eventually saturates at a value. The same holds for the quality factor calculated from the FDTD method. This is shown in Fig. 8(b) for a cavity spacer value $Lc/b = 1$. The FDTD data of Fig. 8(b) are obtained with Bloch boundary conditions applied in the lateral (x) direction. This way one has an infinite source with a plane wave front as in the TMM. The saturation values of the Q-factor for the TMM and FDTD are $\sim$230 and $\sim$250

respectively. This difference might be due to the different ways of calculating the transmission coefficient in the two methods as was mentioned before in Section III.

IV. Conclusion

We have studied the properties of 1-D dielectric cavity structure in a 2-D hexagonal array with the transfer matrix method and the finite difference time domain method. Both methods agree in the position of the defect peak and both yield good agreement (for the peak's position) with the experiment [20] as well. The quality factor though shows sensitivity to a lot of parameters such as the size of the system (both lateral and along the propagation direction), the type of the incoming electromagnetic fields and losses out of the plane of periodicity. In that context the two numerical methods (FDTD and TMM) were compared.

Acknowledgment

The authors would like to thank M. Agio for providing the FDTD code and helpful discussions. They would also like to acknowledge H. Benisty, M. Rattier, and M. Sigalas for helpful discussions.

References

[1] J. D. Joannopoulos, R. D. Meade, and J. N. Winn, *Photonic Crystals: Molding the Flow of Light*. Princeton, NJ: Princeton Univ. Press, 1995.

[2] C. M. Soukoulis, Ed., *Photonic Band Gap Materials*. Dordrecht, The Netherlands: Kluwer, 1996.

[3] ——, *Photonic Crystals an Light Localization in the 21st Century*. Dordrecht, The Netherlands: Kluwer, 2001.

[4] P. R. Villeneuve and M. Piche, "Photonic bandgaps in periodic dielectric structures," *Prog. Quantum Electron.*, vol. 18, pp. 153–198, 1994.

[5] J. D. Joannopoulos, *Photonic Band Gap Materials*, C. M. Soukoulis, Ed., 1996, vol. 315, NATO ASI SERIES E, pp. 1–21.

[6] R. K. Lee, O. Painter, B. Kitzke, A. Scherer, and A. Yariv, "Emission properties of a defect cavity in a two-dimensional photonic band gap crystal slab," *J. Opt. Soc. Amer.*, vol. B 17, pp. 629–633, 2000.

[7] N. M. Lawandy and G.-i. Kweon, "Molecular and free electron spontaneous emission in periodic three dimensional dielectric structures," in *Photonic Band Gaps and Localization*, C. M. Soukoulis, Ed., 1993, vol. B 308, NATO ASI SERIES, pp. 355–368.

[8] S.-Y. Lin, V. M. Hietala, S. K. Lyo, and A. Zaslavsky, "Photonic band gap quantum well and quantum box structures: A high-Q resonant cavity," *Appl. Phys. Lett.*, vol. 68, pp. 3233–3235, 1996.

[9] E. Yablonovitch, "Photonic crystals," *J. Mod. Opt.*, vol. 41, pp. 173–194, 1994.

[10] C. J. M. Smith, T. F. Krauss, H. Benisty, M. Rattier, C. Weisbuch, U. Oesterle, and R. Houdre, "Directionally dependent confinement in photonic-crystal microcavities," *J. Opt. Soc. Amer. B*, vol. 17, pp. 2043–2051, 2000.

[11] C. J. M. Smith, R. M. De La Rue, M. Rattier, S. Olivier, H. Benisty, C. Weisbuch, T. F. Krauss, R. Houdre, and U. Oesterle, "Coupled guide and cavity in two-dimensional photonic crystal," *Appl. Phys. Lett.*, vol. 78, pp. 1487–1489, 2001.

[12] J.-K. Hwang, S.-B. Hyun, H.-Y. Ryu, and Y.-H. Lee, "Resonant modes of two-dimensional photonic bandgap cavities determined by the finite-element method and by use of the anisotropic perfectly matched layer boundary condition," *J. Opt. Soc. Amer. B*, vol. 15, pp. 2316–2324, 1998.

[13] M. M. Sigalas, K. M. Ho, R. Biswas, and C. M. Soukoulis, "Theoretical investigation of defects in photonic crystals in the presence of dielectric losses," *Phys. Rev. B*, vol. 57, pp. 3815–3820, 1998.

[14] H. Hirayama, T. Hamano, and Y. Aoyagi, "Novel surface emitting laser diode using photonic band-gap crystal cavity," *Appl. Phys. Lett.*, vol. 69, pp. 791–793, 1996.

[15] B. Temelkuran, E. Ozbay, J. P. Kavanaugh, G. Tuttle, and K. M. Ho, "Resonant cavity enhanced detectors embedded in photonic crystals," *Appl. Phys. Lett.*, vol. 72, pp. 2376–2378, 1998.

[16] B. Temelkuran, M. Bayidir, E. Ozbay, R. Biswas, M. M. Sigalas, G. Tuttle, and K. M. Ho, "Photonic crystal-based resonant antenna with a very high directivity," *J. Appl. Phys.*, vol. 87, pp. 603–605, 2000.

[17] I. Schnitzer, E. Yablonovitch, A. Scherer, and T. J. Gmitter, "The single-mode light-emitting-diode," in *Photonic Band Gaps and Localization*, C. M. Soukoulis, Ed., 1993, vol. 308, NATO ASI SERIES B, pp. 369–378.

[18] D. F. Sievenpiper, C. F. Lam, and E. Yablonovitch, "Two-dimensional photonic-crystal vertical-cavity array for nonlinear optical image processing," *Appl. Opt.*, vol. 37, pp. 2074–2078, 1998.

[19] M. Agio, E. Lidorikis, and C. M. Soukoulis, "Impurity modes in a two-dimensional photonic crystal: Coupling efficiency and Q factor," *J. Opt. Soc. Amer. B*, vol. 17, pp. 2037–2042, 2000.

[20] M. Rattier, H. Benisty, C. J. Smith, A. Beraud, D. Cassagne, C. Jouanin, T. F. Krauss, and C. Weisbuch, "Perfomance of waveguide-based two-dimensional photonic-crystal mirrors studied with Fabry–Perot resonators," *IEEE J. Quantum Electron.*, vol. 37, pp. 237–243, 2001.

[21] J. B. Pendry, "Photonic band structures," *J. Mod. Opt.*, vol. 41, pp. 209–229, 1994.

[22] J. B. Pendry and P. M. Bell, "Transfer Matrix Techniques for Electromagnetic Waves," in *Photonic Band Gap Materials*, C. M. Soukoulis, Ed., 1996, vol. 315, NATO ASI SERIES E, pp. 203–228.

[23] A. Taflove, *Computational Electrodynamics—The Finite Difference Time-Domain Method*. Norwell, MA: Artech House, 1995.

[24] Z. P. Liao, H. L. Wong, B. P. Yang, and Y. F. Yuan, "A transmitting boundary for transient wave analysis," *Scientia Sinica*, ser. A, vol. XXVII, pp. 1063–1076, 1984.

[25] P. R. Villeneuve, S. Fan, J. D. Joannopoulos, K.-Y. Lim, J. C. Chen, G. S. Petrich, L. A. Kolodziejski, and R. Reif, "Microcavities in channel waveguides," in *Photonic Band Gap Materials*, C. M. Soukoulis, Ed., 1996, vol. 315, NATO ASI SERIES E, pp. 411–426.

Stavroula Foteinopoulou received the B.S. degree in physics from University of Patras, Patras, Greece, in 1995 and the M.S. degree in physics from Rensselaer Polytechnic Institute, Troy, NY, in 1997. She is currently working toward the Ph.D. degree in condensed matter physics at Iowa State University, Ames.

Her research interests are photonic band-gap material structures and left handed materials.

Costas M. Soukoulis received the B.S. degree from the University of Athens, Greece, in 1974, and the M.S. degree and the Ph.D. degree in physics from the University of Virginia from 1978 to 1981.

He was a Research Physicist at Exxon Research and Engineering Company from 1981 to 1984. He has been a faculty member of the Physics Department at Iowa State University, Ames, since 1984. His current research interests include theory of disordered system, light localization, photonic crystals, random lasers, and left-handed materials.